Embedded Micro-channel Cooling Technique to Minimize Thermal Deformation of X-ray and High-power Laser Optics

Embedded Micro-channel Cooling Technique to Minimize Thermal Deformation of X-ray and High-power Laser Optics

Tiwei Wei[1], Lin Zhang[2], Mehdi Asheghi[1], Kenneth E. Goodson[1]

[1]Mechanical Engineering Department, Stanford University, Stanford, CA 94305, USA
[2]LCLS, SLAC National Accelerator Laboratory, 2575 Sand Hill Road, Menlo Park, CA 94304, USA

E-mail: goodson@stanford.edu

Abstract. The thermal deformation of silicon-based X-ray and high-power laser optics is a strong function of the beam power and footprint, mirror geometry as well as the location of the "convective" thermal management solution. Previous research carefully optimized the impact of these parameters and arrived at the "Topside cooling" design concept (smart-cut notches) that reduced the thermal slope error (sub-μrads) by 3-5 orders of magnitude compared to the baseline mirror bottom-side cooling [1,2]. The present work introduces internal embedded microchannel cooling which brings the cooling solution to the close proximity of the laser beam footprint and also reduce thermal spreading. The thermomechanical finite element modelling (FEM) results show that embedded microchannel cooling can reduce the thermal deformation in RMS-Uy by a factor of 40 and 13 compared with topside cooling, for Gaussian distribution beam heat flux with full width half maximum (FWHM) 20 mm and 40 mm, respectively.

1. Introduction

The thermal deformation of silicon-based X-ray and high-power laser optics is a strong function of the beam fluence and footprint, mirror geometry as well as the location of the "convective" thermal management solution. Previous research carefully optimized the impact of these parameters and systematically investigated different indirect cooling solutions, ranging from bottom cooling to full-side cooling and then to topside cooling. The major finding is arrived at the top corner cooling design concept (smart-cut notches) that reduced the thermal slope error (sub-μrads) by 2-3 orders of magnitude compared to the baseline mirror bottom-side cooling [1,2]. However, this cooling design is less effective when the beam footprint is significantly smaller than mirror length. In this paper, we introduce a new cooling design and technique based on internal μ-channel cooling [3] close to the optical surface. The proposed internal μ-channel cooling solution can improve the temperature uniformity by bringing the cooling solution to the close proximity of the laser beam footprint and also reduce thermal spreading. This will minimize the volume of the heated area that can directly impact the thermal deformation, which can reduce thermal slope error by potentially another two orders of magnitudes. In addition, the proposed thermal solution can also provide variable cooling length in the x and y directions to accommodate variable laser footprint, by controlling the cooling channels.

To minimize the thermal deformation in the silicon optics, we systematically investigated the impact of the μ-channel geometry parameters on the displacement normal to the mirror surface along the

beam footprint center (RMS-Uy) utilizing multi-physics thermomechanical and Finite-element-modeling (FEM) analysis. After that, "variable microchannel cooling footprints" is proposed in this paper by controlling the convection cooling channels ON/OFF to match different full width half maximum (FWHM) of the Gaussian distribution heat flux profile. Optimal cooling length is finally provided as a guideline for different FWHM range from 5 mm to 40 mm.

2. Embedded microchannel cooling

As shown in Fig.1(a), the material of the X-ray or high-power laser optics device is chosen as silicon crystal. The size of the silicon-based optics is typically 100 mm long, 50 mm wide with thickness of 50 mm. The illuminated beam footprint is 100 mm long and 2 mm wide on the center of the mirror top surface shown in Fig.1(a)&(c). The mirror is illuminated in the mirror meridional direction with Gaussian power distribution with peak heat flux of 1 W/mm^2 as indicated in Fig.1(b). The investigated FWHM is 5 mm, 10 mm, 20 mm and 40 mm. The embedded internal cooling microchannels are located just beneath the photon beam footprint that reduces the heated volume, resulting in significant reduction in thermal time constant of the system. To understand the thermal deformation and heat transfer behaviors, FEM is performed in the COMSOL 6.0 multi-physical models. The convection liquid heat transfer coefficient is applied across the internal channels surface. Due to the symmetry of the silicon mirror and beam footprint, one-quarter model with symmetric boundary condition is utilized in the simulation.

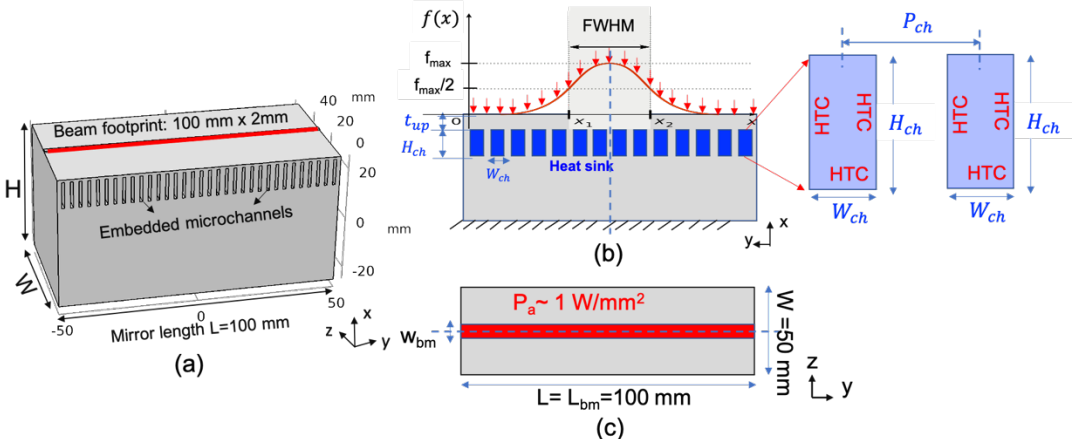

Figure 1: (a) Silicon mirror geometry with embedded microchannel; (b) cross-section view of the microchannel and heat flux distribution profile; (c) top view of the beam heat flux distribution.

2.1. Baseline Uniform Microchannel Cooling

As indicated in Fig.1(b), the channel width is defined as W_{ch}, while the channel pitch is P_{ch} and channel height is H_{ch}. The channel length L_{ch} is kept as 50 mm. The distance between the optics surface to the channel top wall is defined as the t_{up}. In order to understand the channel geometry impact on the vertical displacement and temperature distribution, uniform microchannel cooling corresponding with uniform heat flux heat load distribution is investigated in this section. Optimal channel geometry parameters are chosen based on the trade-off analysis as well as the system constraint and fabrication limits.

2.1.1. 1-D heat transfer analytical model

For the FEM thermomechanical analysis, the heat transfer coefficient is applied alongside the channel internal surface as the convection boundary condition. In order to predict the optical mirror surface temperature and channel pressure drop, a simplified 1-D heat transfer analytical model is developed based on the available frictions and also the channel heat conduction fin analysis. The heat transfer coefficient is determined by the channel geometry dimensions and fluid/thermal boundary conditions, which can be extracted from the available correlations in the literature. For the microchannel

correlations for fanning friction factor from Shapiro, et al. [4] (1954) with hydrodynamic entrance region (developing flow):

$$f_{app} = \frac{1}{Re_{ch}} \times [C \times (L^+)^{-0.5}]; \text{C} = 3.44 \quad (1)$$

The Darcy friction factor for the developing flow is defined as below:

$$f = \frac{\Delta P_{ch} D_h}{2 L_{ch} \rho U_{mean,ch}^2} = 4 * f_{app} \quad (2)$$

For the microchannel correlations for Nusselt number from Bejan, et al. (2004) [5]:

$$\overline{Nu} = C \times (X^+)^{-0.5}; \text{C} = 1.375 \quad (3)$$

Where the L^+ is defined as the dimensionless entrance length $L^+ = \frac{L_{ch}}{Re_{ch} D_h}$, and X^+ is defined as the dimensionless thermal entrance length $X^+ = \frac{L_{ch}}{Re_{ch} Pr D_h}$. The Reynolds number is defined as $Re_{ch} = \frac{\rho U_{mean,ch} D_h}{\mu}$. The Nusselt number is defined as $\overline{Nu} = \frac{h\, D_h}{k}$ while h is the heat transfer coefficient. The D_h is the channel hydraulic diameter. The ΔP_{ch} is defined as the pressure drop between the single channel inlet and outlet. The average channel velocity is defined as $U_{mean,ch}$.

The heat transfer coefficient h can be calculated based on the Nusselt number $\overline{Nu}$ correlation equation (3) while changing the channel dimensions. The mirror surface temperature can be predicted using the 1-D thermal resistance network analysis as well as the fin analysis. The fin width is equal to the channel pitch P_{ch}. Moreover, the pressure drop ΔP_{ch} can be predicted by the equation (1) and (2). The geometry optimization and analysis are all kept under the constant pressure drop condition for practical considerations. To avoid the breakage due to the high liquid pressure, the channel total pressure drop is limited to below 5 bar. The channel aspect ratio H_{ch}/W_{ch} is kept below 5 due to the fabrication limits. For the channel reliability concerns, we keep the channel velocity below 4 m/s to minimize the liquid corrosion issues. Since the 1-D analytical model is assumed constant fluidic properties, the temperature increase of the inlet temperature should be below 2 ℃.

2.1.2. Microchannel geometry optimizations

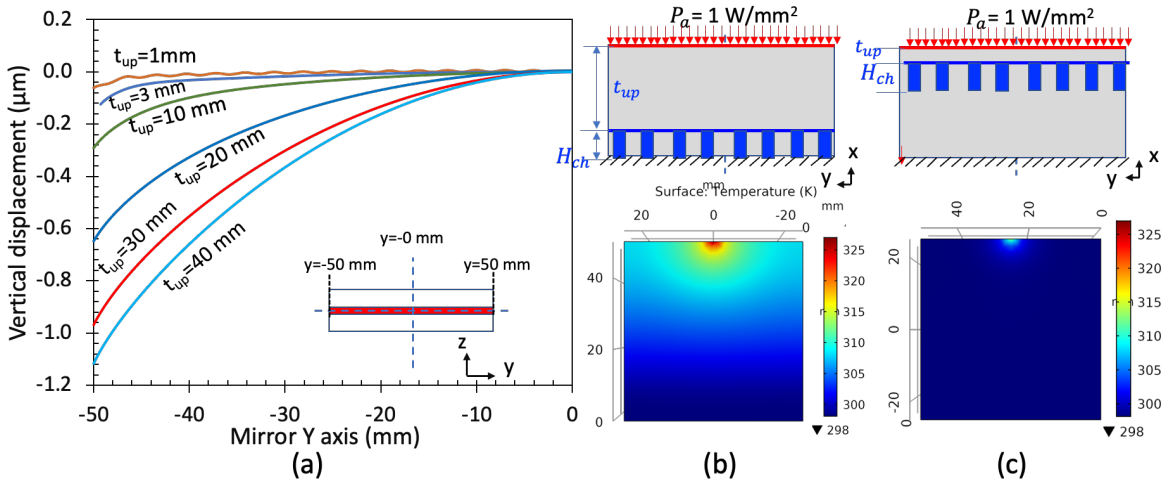

Figure 2: (a) Thermomechanical deformation along the mirror surface under uniform heat flux load; (b) temperature distribution with channels located at the bottom of the mirror t_{up}= 49 mm; (c) temperature distribution with channels located at 1 mm underneath the beam footprint: t_{up}=1 mm. (Uniform heat flux: 1 W/mm^2, T_{in}=298.15K, h = 6785 W/K/m^2, ΔP_{ch}= 0.5 bar, $U_{mean,ch}$ =4.6 m/s, Re_{ch}=1774)

The smaller t_{up} means that the closer the cooling channels to the optics surface. However, if the t_{up} is too thin, the heat spreading across the t_{up} is very limited. As a benchmark, the temperature distribution for the channels located at the bottom of the mirror is plotted in Fig.2(b), where the t_{up} is 49 mm. Compared with channels located at 1 mm underneath the beam footprint (t_{up}=1 mm) shown

in Fig.2(c), it is shown that there is about 43 % of the temperature drop occurs inside the silicon. For t_{up} smaller than 1 mm, temperature "ripples" across the mirror beam heat surface is observed. Therefore, the channel mirror surface temperature is impacted by the microchannel geometry due to the proximity of the cooling channels to the surface (t_{up}=1 mm). As t_{up} increases from 1 mm to 4 mm, there will be an additional thermal resistance due to thicker silicon (between the beam footprint and top of the cooling channel), that results in about 1 °C temperature rise. However, the temperature ripples are reduced as the cooling channel is located deeper inside the silicon mirror. The thermal deformation of the mirror surface is plotted in Fig.2 (a). The results indicate that the optimum location of the cooling channel t_{up} should allow maximum heat conduction spreading in silicon with around 2 mm, which incidentally results in very uniform temperature (ripples ~ 0.01 K) on the laser footprint for all heat transfer coefficient values.

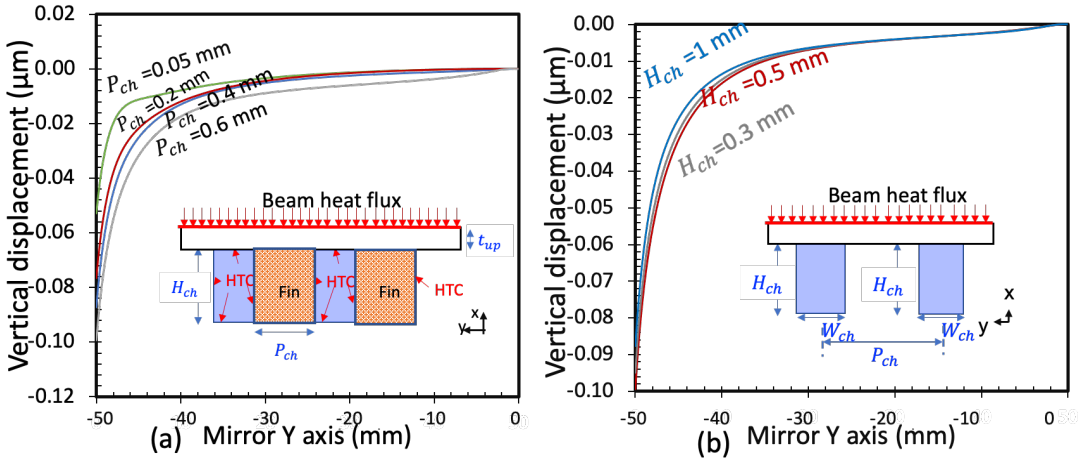

Figure 3: (a) Thermomechanical deformation (vertical displacement) of the mirror surface under different channel pitch; (b) Thermal deformation (vertical displacement) of the mirror surface under different channel height. (Uniform heat flux: 1 W/mm^2, T_{in}=298.15K, ΔP_{ch}= 0.5 bar)

The impact of the channel width, channel pitch and channel height are also investigated in this work. Smaller channel width results in lower mirror optics surface temperature, and therefore smaller vertical displacement and smaller slope error. However, channel pressure drop will increase as the channel width gets smaller. The channel width with 0.2 mm is finally chosen as the optimal. It is found that there is optimal channel pitch for the temperature value, but the temperature varies only 2 °C. As shown in Fig.3(a), smaller channel pitch results in a smaller thermal deformation, as the channel pitch changes from 0.05 mm to 0.6 mm. Considering the structure integrity, 0.2 mm is chosen as the final channel pitch. In addition, large channel height can achieve lower optics surface temperature and smaller thermal deformation. However, with the channel aspect ratio constraint, 1 mm is chosen for the channel height with aspect ratio of 5.

2.2. Variable Beam and Microchannel cooling Footprints

2.2.1. Optimized channel cooling length

In the typical beamline, the FWHM of the Gaussian distribution will be changed for different user condition. Therefore, "Variable microchannel cooling footprints" is proposed in this work by controlling the convection cooling channels ON/OFF to match different FWHM from 5 mm to 40 mm. This approach using variable cooling length to match the different beam footprint length was firstly proposed in 2015 by Zhang et al., for X-ray mirrors [2]. The optimized cooling length could improve the temperature uniformity, and further reduce the mirror thermal deformation, by minimizing the cooling efficiency on the edge, and enhancing the cooling efficiency in the center FWHM region, as shown in Fig.4. To quantify the thermal deformation of the mirror, the room-mean-square (RMS) of the vertical displacement defined as RMS-U_y and RMS value of the residual height error of RMS-dU_y are

calculated. Here the residual height error of dU_y is the differential displacement of Uy and the best spheric fit of the Uy: $dU_y=U_y-U_{y\text{-best spheric fit}}$.

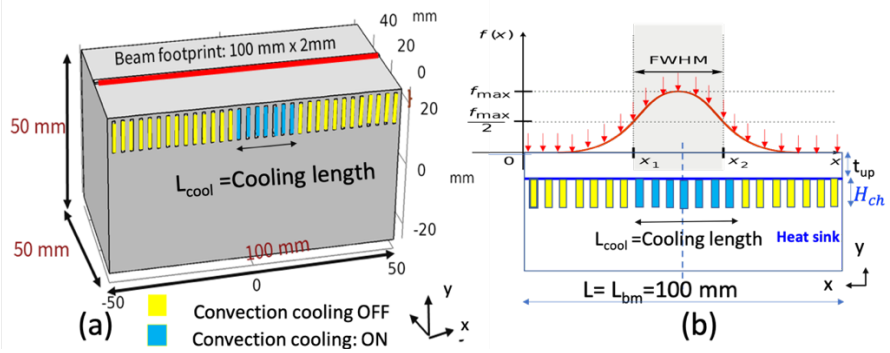

Figure 4: (a) Embedded μ-channel cooling with variable cooling length for the laser optics mirror; (b) Gaussian heat flux distribution profile with matched cooling length.

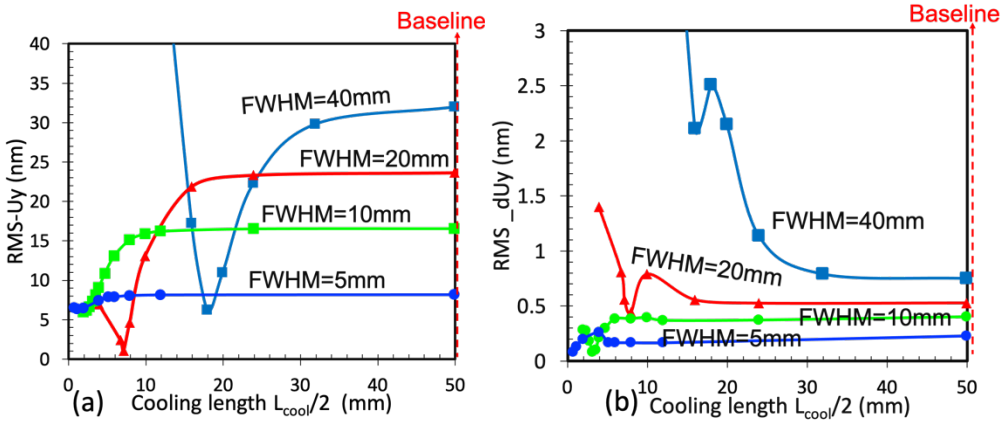

Figure 5: (a) The RMS-U_y (nm) as function of the cooling length for different FWHM; (b) The RMS-dU_y (nm) as function of the cooling length for different FWHM. (Baseline uniform microchannel cooling: $L_{cool}/2$ = 50 mm)

For different FWHM, the optimal cooling length corresponds to the lowest RMS-U_y and RMS-dU_y value in Fig.5. Comparing with baseline uniform microchannel cooling ($L_{cool}/2$ = 50 mm), embedded cooling with optimal cooling length shows significant improvement for larger FWHM = 20 and FWHM = 40 mm. It is shown that the optimal cooling length for FWHM =20 mm is 7.1 mm, while the optimal cooling length is 17.9 mm for FWHM = 40 mm. In addition, optical cooling length with the lowest RMS-dU_y value in Fig.5(b), is mostly located in the longer cooling length. The optimal cooling length for all FWHM from 5 mm to 40 mm is summarized in Table 1 and Table 2.

2.2.2. Benchmarking with different cooling schemes

With the optimized channel cooling length of 7.1 mm for FWHM 20 mm, the embedded microchannel internal cooling solution is compared with the bottom cooling, full-side cooling and also topside cooling. The vertical displacement comparison along the mirror beam direction is shown in Fig.6. Convective heat transfer coefficient with 16000 W/K/m^2 is applied to the bottom cooling, full side cooling and topside cooling configurations. From the FEM modelling, the temperature gradient in the mirror vertical direction is slightly decreased from bottom cooling to full-side cooling, but it remains high temperature gradient. In the case of topside cooling, the temperature gradient is essentially from the mirror center to edges in horizontal direction and in the upper part of the mirror. The temperature gradient in vertical direction (depth) is significantly reduced [1,2]. Embedded cooling with smaller t_{up} = 2 mm could confine the temperature gradient underneath the laser beam footprint shown in Fig.2(c),

resulting in a small thermal deformation. In general, the internal embedded microchannel cooling with optimal cooling length cooling approach can reduce the thermal deformation RMS-Uy by a factor of 40 and 13 compared with the "Topside cooling", for beam FWHM 20 mm and 40 mm, respectively. The optimal cooling length as well as the improvement factor compared with the topside cooling for all FWHM from 5 mm to 40 mm is summarized in Table 1 and Table 2.

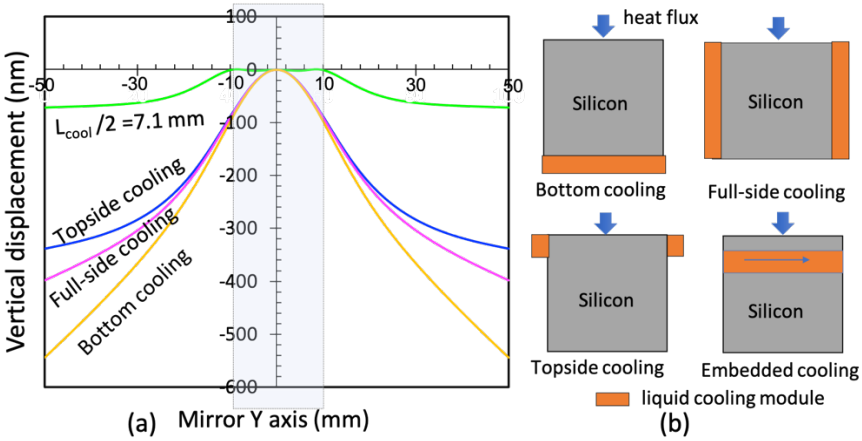

Figure 6: (a) Thermal deformation (vertical displacement) comparison between different cooling schemes; (b) schematics of the bottom cooling, full-side cooling, topside cooling and embedded microchannel cooling with optimal cooling length. (Gaussian heat flux distribution FWHM=20 mm, maximum heat flux = 1 W/mm^2, T_{in}=298.15 K, h = 7829 W/K/m^2, ΔP_{ch}= 0.5 bar, $U_{mean,\,ch}$ =3.4 m/s, Re_{ch}=1155)

Table 1 Cooling comparison of the RMS-U_y (nm) for different FWHM

FWHM	5mm	10mm	20mm	40mm
Embedded cooling with optimal cooling length	6.38	5.96	1.05	6.23
Topside cooling	9.18	20.41	41.06	78.46
Improvement factor	1.43x	3.42x	39x	12.6x

Table 2 Cooling comparison of RMS-dU_y (nm) for different FWHM

FWHM	5mm	10mm	20mm	40mm
Embedded cooling with optimal cooling length	0.08	0.08	0.44	0.75
Topside cooling	0.17	0.36	0.71	1.51
Improvement factor	2.13x	4.5x	1.6x	2x

3. Conclusion

Current results indicate that embedded microchannel cooling of silicon mirror using water as the working fluid with optimized cooling length shows significant improvement comparing with baseline uniform microchannel cooling, especially for larger FWHM value. The present work also shows that this cooling approach can reduce the thermal deformation RMS-U_y by a factor of 40 and 13 compared with the "Topside cooling", for beam FWHM 20 mm and 40 mm, respectively.

References

[1] Zhang, L., et al., 2012, Journal of Physics: Conference Series 425 (2013) 052029.
[2] Zhang, L., et al., 2015. J. Synchrotron Radiat, 22(5), pp.1170-1181.
[3] Jung, K.W., et al., 2019, Int. J. Heat Mass Transf.. Vol. 130, pp. 1108-1119.
[4] Shapiro, A., et al., Proc. of US Second National Congress of Applied Mechanics, pp. 733– 741, ASME, New York, NY, 1954.
[5] Bejan, A., Kraus, A.D., Heat transfer handbook, John Wiley & Sons (2003)